Journal of Applied Polymer Science

Silver nanoparticle incorporated poly(L-lactide-*co*-glycolide) nanofibers: Evaluation of their biocompatibility and antibacterial properties

Aleksander Góra,[1] Molamma P. Prabhakaran,[1] Goh Tze Leng Eunice,[2] Rajamani Lakshminarayanan,[2,3] Seeram Ramakrishna[1]

[1]Center for Nanofibers and Nanotechnology, Department of Mechanical Engineering, National University of Singapore, 2 Engineering Drive 3, 117576 Singapore, Singapore

[2]Anti-Infectives Research Group, Singapore Eye Research Institute, Singapore 168751, Singapore

[3]Duke-NUS SRP Neuroscience and Behavioural Disorders, Singapore 169857, Singapore

Correspondence to: M. P. Prabhakaran (E-mail: nnimpp@nus.edu.sg)

ABSTRACT: The objective of this work is the fabrication of poly(L-lactide-*co*-glycolide) or PLGA (with LA/GA ratios of 50/50 and 75/25) nanofibers containing silver nanoparticles (AgNPs) by the method of electrospinning. The incorporation of AgNPs in PLGA was carried out in three different concentrations (1, 3, 6 w/w %).The electrospun nanofibers were evaluated for their morphology by scanning electron microscopy and their fiber diameters ranged between 487 and 781 nm. Integration of AgNPs within the fibers was verified by spectroscopy studies, while the mechanical properties of the developed fibers were found comparable to the mechanical properties of the human skin. Proliferation of human dermal fibroblasts (HDF) demonstrated minimal cytotoxicity on fibers containing 1 wt % and 3 wt % of AgNPs, while 6 wt % of AgNPs inhibited cell proliferation. Antimicrobial activity was studied using three different strains of Gram-positive and Gram-negative bacteria. Results of the HDF proliferation and antimicrobial studies showed that the electrospun PLGA75/25 containing 3 wt % AgNP can function as a suitable substrate for wound dressing, compared to the other scaffolds of this study. © 2015 Wiley Periodicals, Inc. J. Appl. Polym. Sci. **2015**, *132*, 42686.

KEYWORDS: biocompatibility; biomaterials; biomedical applications

Received 16 March 2015; accepted 23 June 2015
DOI: 10.1002/app.42686

INTRODUCTION

Polymeric nanofibrous scaffolds can function as a tissue engineered skin graft for the treatment of wounds, burns, or post-surgical scars. Regenerative medicine using bioengineered grafts are widely investigated with the aim of bringing new solutions for current issues in medical care. At the same time, microbial infections are the most common complications associated with medical surgeries and wound management regimen. The presence of antibacterial and bioactive materials such as the antibiotics,[1,2] metal particles,[3,4] or medicaments,[5–7] within the polymeric nanofibrous scaffolds could minimize the risk of microbial infections as well as support the cell recruitment and growth.[8] Surgical site infections (SSI) which occurs in 0.5–15% of all hospitalized patients, depend on the type of operation carried out, and affect around 1.4 million people annually world wide.[9] In the early stages of wound healing, neutrophils accumulate inside the wound to prevent bacterial film creation, nevertheless this process is often "in efficient" and biofilm formation prevents re-epithelialization of the tissue. Resistance to neutrophils developed by bacterial biofilm transforms the relatively harmless acute wound into dangerously chronic wound.[10] Various polymeric systems have been investigated in the field of skin tissue engineering. Natural polymers like collagen, gelatin, or fibrin[11,12] showed good biological properties but they lack sufficient mechanical properties to support the regeneration of the skin tissue. Synthetic polymeric materials investigated in this field, include polypropylene, polyvinyl alcohol, or polyethylene glycol,[13–15] provide sufficient mechanical strength but without any natural antibacterial properties. Nanofibrous scaffolds shows extraordinary mechanical resistance with very high surface energy and morphology similar to the natural extracellular matrix of human skin.[16] Materials in fibrous architecture create a unique mesh of micro or sub-micro pores which allow the cells to attach, communicate, and support the exchange of nutrients and metabolites. After implantation, the scaffolds slowly degrade with time, such that the natural tissue gets sufficient amount of time to replace the synthetic polymeric mesh and recreate the tissue, while disintegrating to neutral compounds which are naturally processed by the human body.[17]

Poly(lactide-*co*-glycolide) (PLGA) is one of the aliphatic biodegradable polymers widely investigated in the field of healthcare and regenerative medicine.[18] PLGA degrades safely within the

biological system through hydrolytic degradation and the rate of degradation can be controlled by the ratio of their monomers, namely the lactide and the glycolide.[19,20] In recent years, polymers incorporated with metal nanoparticles gained much attention, thanks to surface modification techniques and better understanding of its biological, magnetic, and electric properties.[21,22] Silver nanoparticles (AgNPs) incorporated in polymeric foams showed antibacterial properties against Gram-negative and Gram-positive bacteria[23,24] while high concentrations of AgNPs in the matrix have even been demonstrated to show anti-cancer properties.[3] The mechanism of antibacterial properties of AgNPs is still not fully understood, however, it was hypothesized, that it causes cell lysis or inhibit cell transduction.[25] Combining the nanofibrous biodegradable matrix with antibacterial properties of AgNPs is a novel approach toward the fabrication of functionalized scaffold matrix for skin tissue engineering or as implantable wound dressings, to solve the problem of increasing number of SSI. In this study, we investigated two polymeric systems as potential materials for wound healing. PLGA with lactide : glycolide ratio of 50 : 50 and 75 : 25 was individually incorporated with AgNPs to obtain nanofibrous composites by electrospinning technique. The optimization of the electrospinning process was carried out, and the evaluation of mechanical and structural properties of the developed fibers along with their cellular biocompatibility was investigated during this study. Further, the antibacterial properties of the scaffolds against the Gram-positive and Gram-negative bacterial strains: *Staphylococcus saprophyticus, Klebsiella pneumoniae, Pseudomonas aeruginosa,* and *Escherichia coli* were conducted to investigate the potential of utilizing these nanofibrous scaffolds as novel wound dressings.

MATERIALS AND METHODS

Materials

Poly(L-lactide-*co*-glycolide) with L : G ratio of 50 : 50 (B6010-2, PLGA 50/50) and 75 : 25 (B6007-1, PLGA 75/25) both with an inherent viscosity of 0.55–0.75, were purchased from LACTEL Absorbable Polymers (Durect, Birmingham, AL). Dimethylformamide (DMF), chloroform, phosphate buffer saline (PBS), AgNPs (TEM confirmed size < 100 nm, no.658804), Dulbecco's Modified Eagle's Medium (DMEM), and penicillin-streptomycin antibiotic solution were purchased form Sigma-Aldrich (St. Louis, MO). Fetal bovine serum (FBS) and Trypsin (10×) were purchased from Gibco (Life Technologies, United Kingdom) and AlamarBlue BUF012B Cell Viability Assay reagent was purchased from AbDSerotec (Kidlington, United Kingdom). Human dermal fibroblasts (HDFs) were purchased from ATCC (Manassas, VA) and used for the biocompatibility studies. Bacterial strains used for the experiments were purchased from ATCC (Manassas, VA). Four Gram-positive strains: *S. saprophyticus* (strain codes: 15305, BAA-750, 49907, 49453) and four Gram-negative strains: *K. pneumoniae* (DM4299), *E. coli* (16027R), *P. aeruginosa* (23155 and 4299) were used for the antibacterial evaluation.

Electrospinning of PLGA-Based Nanofibrous Scaffolds

Electrospinning of PLGA 50 : 50, PLGA 75 : 25, and AgNPs incorporated PLGA nanofibers were carried out during this study. The polymers were individually dissolved in a mixture of chloroform and DMF (3 : 1) at a concentration of 25% (wt/v) for PLGA 50/50 and 20% (wt/v) for PLGA 75/25, respectively. For preparation of the composite nanofibers, first the nanoparticles were added to the above solvent mixture at concentrations of 1, 3, and 6% (wt/v) with respect to the concentration of PLGA, and stirred for 24 h by magnetic stirrer followed by ultrasound stirring (FB505, Fisher Scientific, Hampton, NH) for 20 min in 30 s intervals. Further, the polymer (either PLGA 50 : 50 or PLGA 75 : 25) was added and the whole mixture was stirred for 12 h period. Custom made electrospinning equipment used for this study consists of a high voltage power supply (Gamma High Voltage Research, FL), syringe pump (KDS100, KD Scientific, Holliston, MA), and a flat lab jack as the collector. Polymer solution was loaded into 5 mL syringe and attached with a 25 G (0.51 mm) blunt needle (Dickinson and Company, NJ), which was further connected to high voltage power supply. The distance between the needle tip and collector was maintained at 12 cm. The flow rate of the solutions ranged from 0.5 to 1.5 mL/h, while the applied electric potential ranged from 10 to 18 kV. Nanofibers were collected on aluminum foil covered jack, and dried in vacuum for 24 h prior to characterization. For cytotoxicity and antibacterial studies, the scaffolds were sterilized under UV lamp for 30 min.

Surface, Chemical, and Mechanical Characterization of the Fibers

Electrospun fibers were examined under the scanning electron microscope (SEM; JEOL JSM-6010LV, Tokyo, Japan) after sputter coating with gold (JEOL JFC-1200 coater, Tokyo, Japan). Fiber diameter was measured from the SEM images by application of the ImageJ software (National Institutes of Health, USA),[26] and around 80–100 measurements per sample was performed. The best optimized parameters for electrospinning was identified upon obtaining uniform, beadless, and random fibers.

Atomic Force Microscope (Nanowizard 3, JPK, Germany) was used to measure the surface roughness of the scaffolds. Cantilever of nominal stiffness of 5 N/m (TAP-150G, Budget Sensors, Bulgaria) was used for imaging in tapping mode. AFM image measurements were done at three areas of size 20 × 20 μm with resolution of 1024 × 1024 pixels which means that every average values for single image was based on 1024 roughness profiles. Three areas per sample were measured and the average roughness values were calculated.

Hydrophobicity/hydrophilicity properties of the electrospun nanofibers was measured by Water Contact Angle system (VCA Optima Surface Analysis, AST Products, Billerica, MA), averaged from 10 individual measurements per sample. Each measurement was done by using 10 μL of ultrapure water. Camera pictures were taken within 10 s after the water drop touched the scaffolds, and the contact angle measurement was carried out. Fourier transform infrared spectroscopy (FTIR) measurements were done using Avatar 380 FTIR Spectrometer (Thermo Nicolet, Waltham, MA) over a range of 400–4000 cm^{-1} at a resolution of 2 cm^{-1}.

Mechanical properties of the scaffolds were determined using a Universal Tensile Machine (Instron 5943, USA). The electrospun mats were cut into rectangular shapes (10 × 20 mm) and placed in UTM load cell with a maximum load of 250 N.

Thickness of each specimen was measured using digital micrometer (Multitoyo, Japan) and ranged between 80 and 100 μm. Samples were stretched at a rate of 10 mm/min until they complete break. Tensile strength and Young's modulus (YM) were obtained from the stress-strain curve drawn for each scaffold.

Concentration of AgNPs within the electrospun scaffolds was tested by UV-VIS spectrophotometer (UV-3600, Shimadzu, Japan). In order to do this, 2 mg of nanofibrous sheets were individually dissolved in a mixture of chloroform and DMF at appropriate ratios, such that an amount of 1 mg per mL of solution was obtained. After complete dissolution of the polymer and NPs, the mixture was stirred for 10 s with ultrasound mixer to break possible agglomerates of AgNPs and used for UV-Vis measurements. Mixture of chloroform and DMF at a ratio of 3 : 1 served as the reference during the UV-Vis study.

Culture of Human Dermal Fibroblast and Cytotoxicity Test

HDF was cultured in complete medium that contained DMEM with 10% FBS and 1% antibiotic mixture and grown in a 75 cm^2 culture flask. Cells were incubated for 6 days in incubator under humidified atmosphere at 37°C and 5% CO_2. Culture media was changed once every 3 days. Once the cells reached confluency, they were trypsinized, counted by hemocytometer, and used for the assays.

To study the cell proliferation, the nanofiber spun on cover slips (diameter of 15 mm) were placed in 24 well plate and metal ring was placed on top of the scaffold. Scaffolds, rings, and well plates were pre-sterilized under UV light before using them. The scaffolds placed in 24 well plates were washed thrice with phosphate-buffered saline (1× PBS) and incubated overnight with complete culture medium in 37°C. Approximately 10,000 cells/well were seeded on the each scaffold for cell viability test. In order to establish the calibration curve for cell viability assay, cells were also seeded in separate wells at a count of 10,000, 20,000, 40,000, 80,000, 160,000, and 320,000 cells/well.

The proliferation of cells on the scaffolds were evaluated by AlamarBlue® assay. The assay is commonly utilized to measure the proliferation of various human and animal cell lines, bacteria, or fungi, quantitatively. The cell viability assays were performed at four different time points (2, 4, 6, and 8 days). On designated time periods, a 10% solution of AlamarBlue® in complete media was used to replace the media in culture well plates and kept for incubation for 4 h at 37°C. After incubation, 100 μL of the media containing AlamarBlue® was transferred into 96 well plates and the measurement was performed using a spectrophotometric plate reader (Varioscan Flash, Thermo Scientific, Fisher Scientific, Hampton) with excitation and emission wavelength of 545 nm and 590 nm, respectively. In this test, cells viability is based on resazurin, a non-toxic, cell permeable compound which is being reduced by living cells to resorufin, which is fluorescent red in color. Blank wells without cells but with AlamarBlue® solution was also used to minimize error. Calibration curve was drawn by measuring the intensity of emission for 10,000, 20,000, 40,000, 80,000, and 120,000 cells seeded and incubated for 12 h at 37°C. The curve linear fit to obtain a straight line and was later used to calculate the cell viability on each scaffold.

Antibacterial Properties of the Scaffolds

The antibacterial activity of the developed scaffolds was tested against four Gram-negative *K. pneumonia* (DM4299), *E. coli* (16027R), and *P. aeruginosa* (23155 and 4299) and four Gram-positive strains of *S. saprophyticus* (15305, BAA-750, 49907, 49453). The bacterial cultures were grown overnight in Tryptic Soy Agar at 37°C. A few colonies were inoculated to a turbidity of 0.5 McFarland standard and swabbed uniformly across a Mueller-Hinton agar (MHA) plate which contains 30.0% beef infusion, 1.75% casein hydrolysate, 0.15% starch, and 1.7% agar with pH adjusted to neutral at 25°C. The scaffolds (size: 0.5 × 0.5 cm^2) were placed on the surface of the MHA plate. In order to determine the antibacterial property of AgNPs (positive control), 2 mg of the AgNPs was dispersed in 1 mL of water for injection and 100 μL was added on the surface of the MHA plate. All the culture plates were placed in 37°C incubator and the zone of clearance was measured after 24 h with photos taken, and the experiments were performed in duplicates.

RESULTS AND DISCUSSION

Optimization of the Electrospinning Process and SEM Analysis

Optimization of the electrospinning process was carried out to obtain continuous and uniform nanofibers. PLGA50/50-NP0 was electrospun under a high electric potential of 15 kV and the flow rate was maintained at 0.5 mL/h. PLGA50/50 incorporated with AgNPs (1 wt %, PLGA50/50-NP1; 3 wt %, PLGA50/50-NP3; 6 wt %, PLGA50/50-NP6) were produced under 12 kV of electric potential at a flow rate of 1 mL/h. PLGA75/25-NP0 mats were electrospun at an electric potential of 15 kV and 1 mL/h, while 10 kV with 1 mL/h flow rate was used for electrospinning the nanoparticle containing PLGA75/25 fibers (PLGA75/25-NP1, PLGA75/25-NP3, PLGA75/25-NP6). SEM images showed bead-less nanofibers in the nanoscale range with uniform distribution of fiber diameters. The fiber diameter of PLGA75/25-NP0 was found higher than the fiber diameter of PLGA50/50-NP0. Incorporating AgNPs into the polymer matrix greatly increase the electrical conductivity of the polymer solution, thus influencing the minimal potential required to create a Taylor cone and overcome the surface tension of the liquid,[27] which results in decreased fiber diameter for the AgNPs incorporated PLGA50/50 and PLGA75/25 scaffolds (Figure 1).The fiber diameter of PLGA50/50-NP0 decreased from 612 ± 144 nm to 487 ± 67 nm when a maximum amount (6 wt %) of AgNPs was added. For the PLGA75/25-NP0 composites, the fiber diameter reduced from 781 ± 130 nm for PLGA75/25-NP0 to 538 ± 72 nm for PLGA75/25-NP6 scaffolds. The increase in the electrical conductivity of polymer solution with incorporation of salts or particles were previously demonstrated by Angammana *et al.*,[28] where they found that the fiber diameter decreased from 250 to 150 nm with incorporation of NaCl to aqueous polyethylene oxide solution. This might have also occurred during our studies, such that the fiber diameter of AgNP incorporated PLGA scaffolds was lower than their respective pure PLGA scaffolds. However, an increase in the concentration of AgNPs did not cause further reduction in the fiber diameter of the scaffolds.

Atomic Force Microscopy

Atomic force microscopy measurements revealed the nanofibrous three-dimensional structure of the scaffold (Figure 2) and

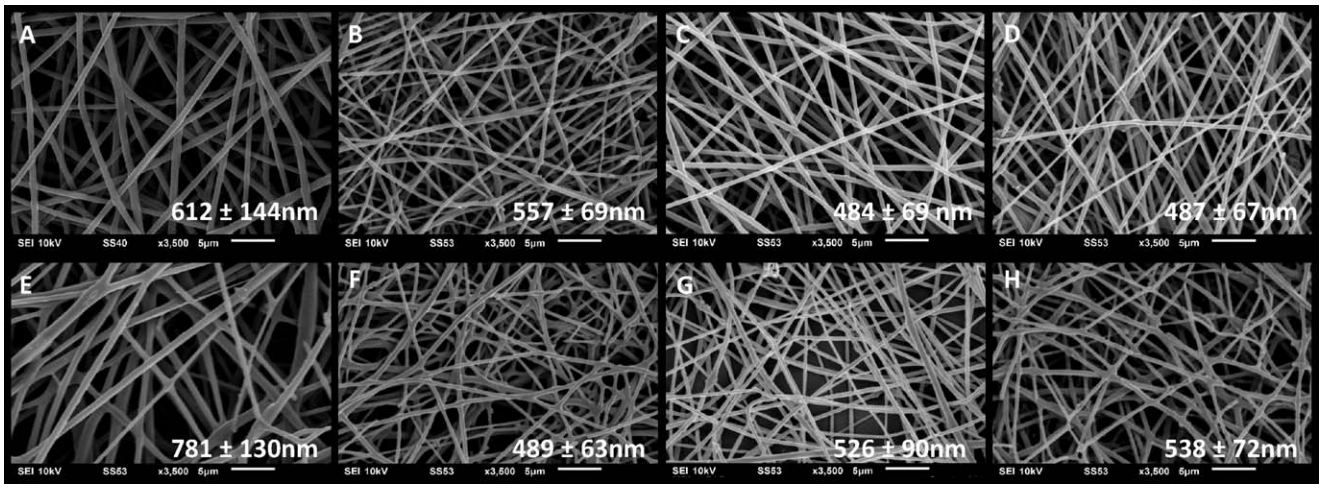

Figure 1. SEM images of electrospun fibers with their diameters: (A) PLGA50/50-NP0, (B) PLGA50/50-NP1, (C) PLGA50/50-NP3, (D) PLGA50/50-NP6, (E) PLGA75/25-NP0, (F) PLGA75/25-NP1, (G) PLGA75/25-NP3, and (H) PLGA75/25-NP6.

the images were used to calculate the surface roughness of the scaffolds. Roughness of the scaffolds were calculated based on the average values for every scanning line in the area and two different values of roughness have been presented (Figure 3). Average Roughness (Ra) is defined as the average value of roughness profile, while Root Mean Square Roughness (Rq) is defined as the root mean square average of the roughness profile. Compared to PLGA50/50-NP0, the average surface roughness (Ra) of PLGA50/50-NP6 scaffolds, decreased from 854 ± 15 nm to 510 ± 69 nm. RMS roughness (Rq) for PLGA50/50-NP6 was obtained as 634 ± 59 nm, while those of PLGA50/50-NP0 was measured as 1055 ± 14 nm. For PLGA75/25 scaffolds, the decrease in roughness was gradual from a value of 841 ± 21 nm (Ra) and 1038 ± 22 nm (Rq) for PLGA75/25-NP0, leading to 322 ± 51 nm (Ra) and 423 ± 47 nm (Rq), respectively, for PLGA75/25-NP6. Similar to the results of our SEM analysis, the roughness of the fibers reduced with the decrease in the fiber diameter, such that they became smoother with the increase in the amount of nanoparticles incorporated within the PLGA matrix.

Wettability

Wettability test was carried out for all the scaffolds prepared during this study. Every sample was tested 5–8 times with a drop water volume of 10 μL. The PLGA50/50-NP0 and PLGA75/25-NP0 scaffolds showed hydrophobic surface with a contact angle of around 130°. Addition of nanoparticles changed the hydrophobicity of the composite scaffolds to $126 \pm 2°$, $125 \pm 3°$, and $124 \pm 1°$, respectively, for PLGA50/50-NP1, PLGA50/50-NP3, and PLGA50/50-NP6. A similar trend was also observed for the AgNPs containing PLGA75/25 scaffolds. Figure 4 shows the trend in contact angle values for the different scaffolds of this study. No significant differences in the contact angle between the scaffolds were observed, suggesting that the AgNPs did not influence the hydrophobicity of the scaffold.

Fourier Transform Infrared Spectroscopy

The obtained spectra suggests that the addition of nanoparticles into the polymer matrix did not lead to significant changes in the chemical composition of the composite scaffolds. Intensities

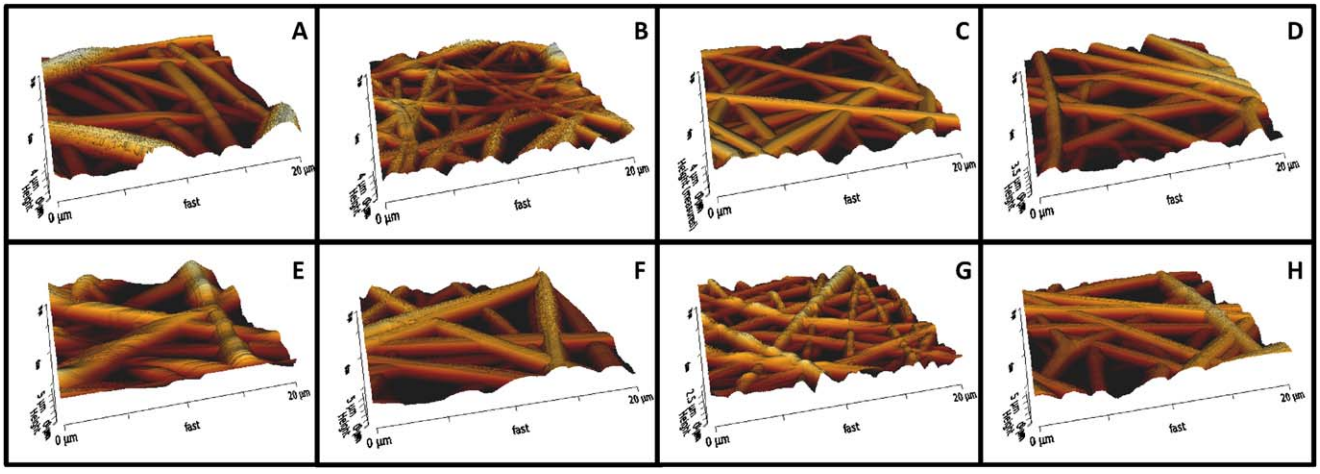

Figure 2. AFM pictures of the developed nanofibrous scaffolds (A) PLGA50/50-NP0, (B) PLGA50/50-NP1, (C) PLGA50/50-NP3, (D) PLGA50/50-NP6, (E) PLGA75/25-NP0, (F) PLGA75/25-NP1, (G) PLGA75/25-NP3, and (H) PLGA75/25-NP6. [Color figure can be viewed in the online issue, which is available at wileyonlinelibrary.com.]

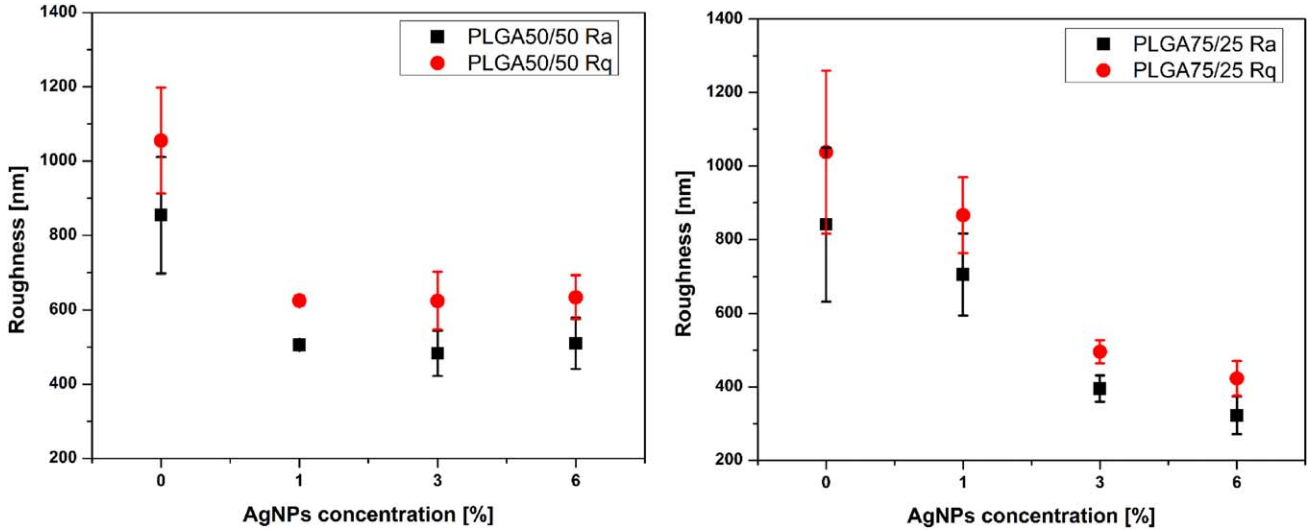

Figure 3. Average roughness (Ra) and Root Mean Square Roughness (Rq) of the electrospun nanofibrous scaffolds as determined by AFM analysis. [Color figure can be viewed in the online issue, which is available at wileyonlinelibrary.com.]

and localization of peaks did not change drastically with increased amount of AgNPs.[29] Peaks around 1470 cm^{-1} showed sharper decrease of transmittance for polymeric systems with AgNPs. Bands observed in the region around 1753 cm^{-1} are due to the stretching of carbonyl groups from PLGA, while peaks between 2944 and 2995 cm^{-1} shows the stretching vibrations of —CH, —CH_2, —CH_3 groups of PLGA. Also the peaks observed between 1250 and 1500 cm^{-1} (1268, 1382, and 1452 cm^{-1}) represent the deformation vibrations of the same groups. The peaks in the range of 1300–1150 cm^{-1} represents ester (C—O)stretching vibrations as well as wagging vibrations of —CH_2 and —CH (1270 and 1184 cm^{-1}).[30] No significant differences between the infrared spectral images of PLGA50/50 and PLGA75/25 was observed, and such details were also reported by Taheri *et al.*,[29] nevertheless higher lactide content might be distinguished by the sharper peak observed at around 750 cm^{-1} along with a high intensity peak at around 1145 cm^{-1}. Absence of peaks in the range of 3600–3400 cm^{-1} suggests the lack of hydroxyl groups, demonstrating that the polymer remained anhydrous (Figure 5).

UV-VIS Spectroscopy

With different concentrations of AgNPs incorporated in different scaffolds, an evaluation on the amount of NPs that actually got incorporated within the scaffold was determined qualitatively. According to Beer-Lambert law, the absorbance of a solution is directly proportional to the concentration of the absorbing compound and hence this method can be used to analyze the concentration of compound in solution at a fixed path length. Increased absorbance with increasing amount of nanoparticles suggests increasing amounts of nanoparticles within the polymer matrix. Peaks in the range of 390–420 nm

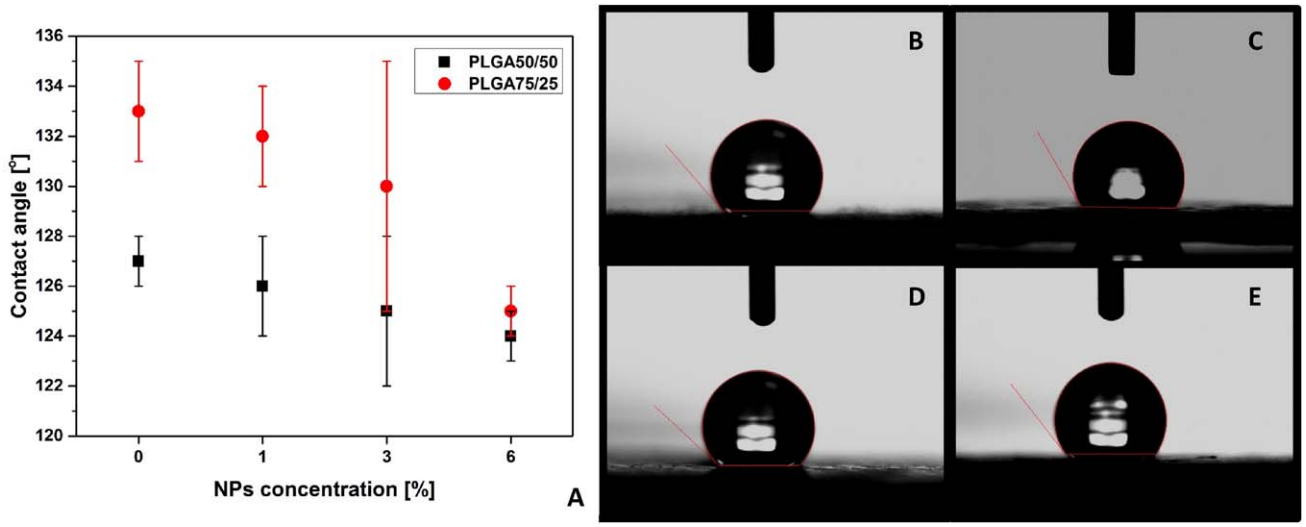

Figure 4. (A) Change in contact angle of the scaffolds in response to the increased incorporation of AgNPs; and a comparative representation of the contact angle values for (B) PLGA50/50-NP0, (C) PLGA50/50-NP6, (D) PGLA75/25-NP0, and (E) PLGA75/25-NP6. [Color figure can be viewed in the online issue, which is available at wileyonlinelibrary.com.]

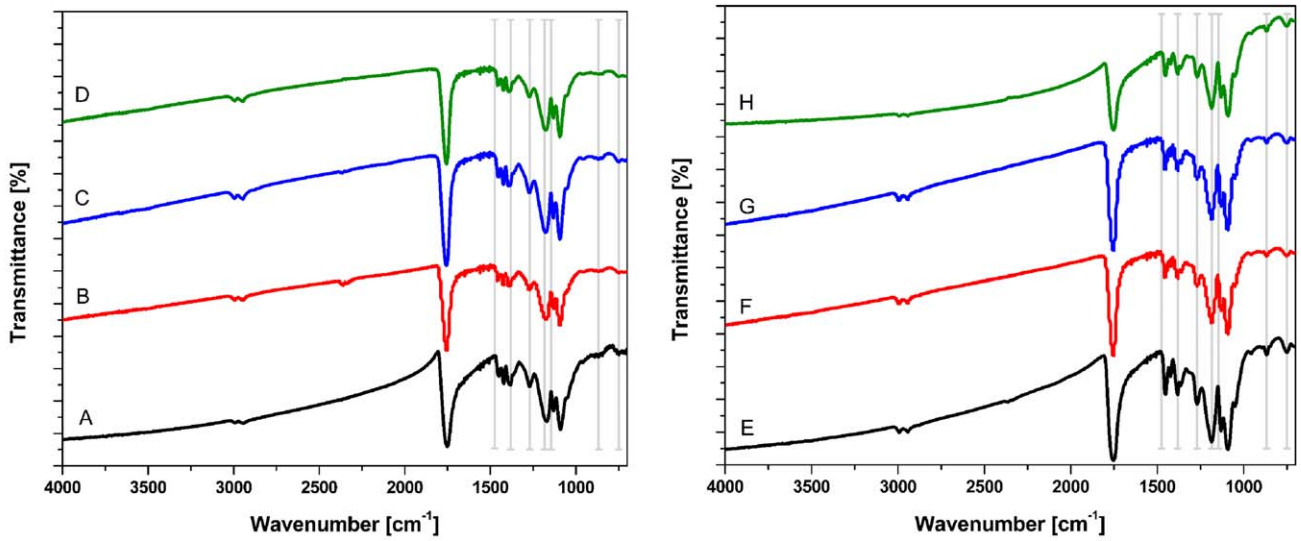

Figure 5. FTIR spectra of the developed electrospun scaffolds (A) PLGA50/50-NP0, (B) PLGA50/50-NP1, (C) PLGA50/50-NP3, (D) PLGA50/50-NP6, (E) PLGA75/25-NP0, (F) PLGA75/25-NP1, (G) PLGA75/25-NP3, and (H) PLGA75/25-NP6. [Color figure can be viewed in the online issue, which is available at wileyonlinelibrary.com.]

are characteristic of AgNPs.[31–33] An increase in the intensity of the peaks was observed with increasing incorporation of AgNPs, with the highest peak intensity was observed for PLGA composites incorporated with 6 wt % of particles (Figure 6).

Mechanical Properties of the Electrospun Scaffolds

Figure 7 shows the stress-strain curves of the different scaffolds obtained during this study. Maximum tensile strength of 4.83 ± 0.27 MPa was measured for pure PLGA75/25-NP0 scaffolds and it decreased to 2.55 ± 0.95 MPa for PLGA75/25-NP6. On the other hand, PLGA50/50-NP0 showed lower ultimate tensile strength of 1.65 ± 0.11 MPa and it decreased to 0.71 ± 0.11 MPa for PLGA50/50-NP6. YM was calculated from the slope of the linear part of the initial strain by the method previously reported.[34,35] YM was found highest for PLGA75/25-NP0, and lowest for PLGA75/25-NP6 scaffold. Details of the ultimate tensile stress, ultimate tensile strain, and YM of the different scaffolds are presented in Table I. The differences in the molecular weight of PLGA75/25-NP0 and PLGA50/50-NP0 might be attributed to the significant decrease in YM of these scaffolds, measured, respectively, as 191.29 ± 14.85 and 58.00 ± 8.31 MPa (Figure 7). Introduction of AgNPs decreased the stiffness of PLGA75/25-NP6 scaffold by 41% compared to pure PLGA75/25-NP0, while 62% reduction in stiffness was observed for the PLGA50/50 counterparts.

Proliferation of HDF on the Electrospun Scaffolds

HDF proliferation on the scaffolds was determined by Alamar-Blue™ assay during day 2, 4, 6, and 8. Calibration curve was obtained after seeding a known amount of cells in 24-well plate and the measurement was taken approximately 12 h post-seeding. Linear fitting of the calibration curve was performed and this was used to estimate the number of cells present on the scaffolds. TCP served as the control during the cell proliferation study. The number of cells was found to increase during

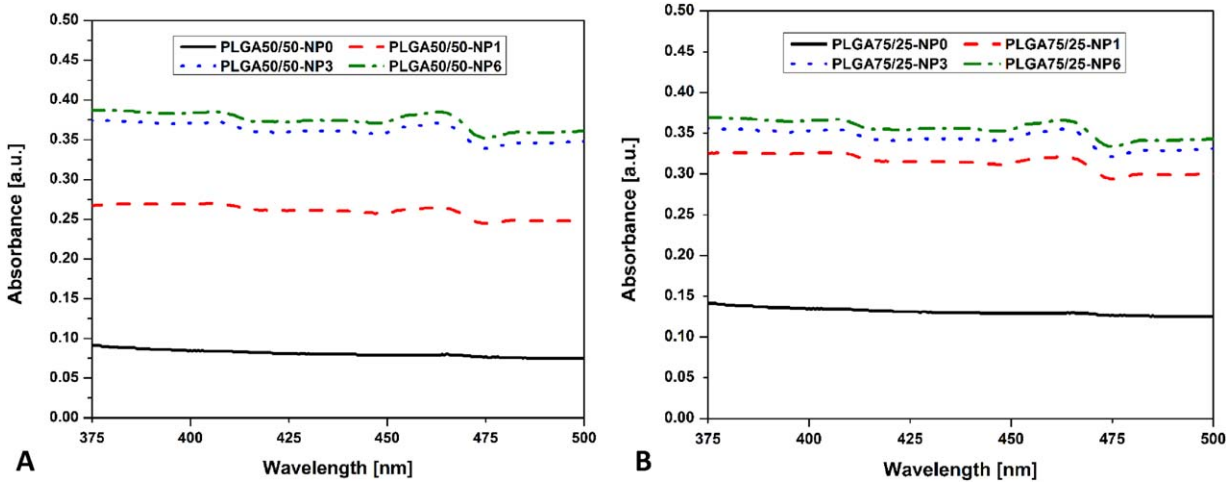

Figure 6. UV-VIS absorption spectra of PLGA-AgNPs nanofibers after dissolution in $CHCl_3$/DMF. [Color figure can be viewed in the online issue, which is available at wileyonlinelibrary.com.]

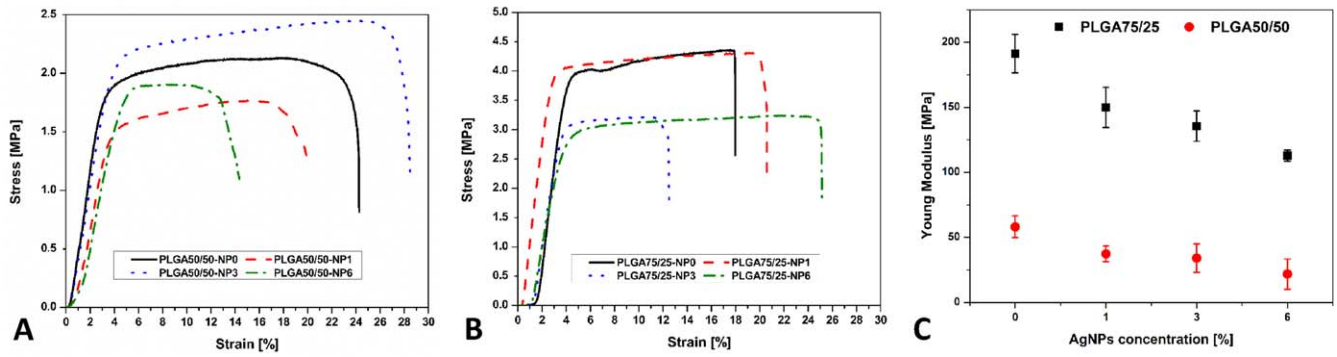

Figure 7. Stress-strain curves obtained for (A) PLGA50/50 and (B) PLGA75/25 related scaffolds; (C) trend in YM of the developed scaffolds with respect to the amount of AgNPs incorporated. [Color figure can be viewed in the online issue, which is available at wileyonlinelibrary.com.]

the cultivation time on all scaffolds. On day 8, cells grown on TCP showed higher proliferation rate of approximately 11.6% and 16.5% higher than PLGA75/25-NP0 and PLGA50/50-NP0, respectively (Figure 8). Our cell proliferation studies showed that an incorporation of 1 wt % of AgNPs did not cause any negative cell response and the proliferation rate was similar to that of the pure polymer matrix. Further increase in the concentration of the nanoparticles caused an increase in the cell proliferation on PLGA75/25-NP3 and PLGA50/50-NP3 scaffolds. On day 8, the increase in cell proliferation was 36.8% and 27.8% higher on PLGA50/50-NP3 and PLGA75/25-NP3 scaffolds compared to the cell growth on respective scaffolds on day 6. However, the incorporation of 6 wt % of nanoparticle was found toxic to fibroblast cells, and it hindered the cell growth on both PLGA75/25-NP6 and PLGA50/50-NP6 scaffolds.

Antibacterial Activity of PLGA-NPs

Antibacterial activity was measured against four types of bacteria: *K. pneumoniae*, *E. coli*, *P. aeruginosa*, and *S. saprophyticus*. Three different strains of *S. saprophyticus* and two different strains of *P. aeruginosa* were also used for this study. Bacteria free area was measured as the zone of inhibition for both Gram-positive and Gram-negative bacteria, in order to determine the potential of antibacterial activity of the scaffolds. Pure PLGA nanofibrous mat was used as the negative control, while 1 mg of AgNPs itself served as the positive control. No antibacterial activity was observed for PLGA50/50-NP0 and PLGA75/25-NP0 nanofibers, while higher concentration of AgNPs within the composite scaffolds enhanced the antibacterial properties of the scaffolds (Figure 9).

Due to the presence of higher concentrations of the antibacterial agent (AgNPs), the positive control showed significantly larger bacteria free circles in all cases from 0.8 cm for *E. coli* (16027R) and *P. aeruginosa* (PA23155); and up to 2.3 cm for *S. saprophyticus* (SS49907). For the PLGA50/50, the antimicrobial activity ranged from 0.4 cm (PLGA50/50-NP1) and went up to 1.2 cm (PLGA50/50-NP6) for Gram-positive *S. saprophyticus* (SS15305 and SS49907). For Gram-negative bacteria, this ranged from 0.5 cm (PLGA50/50-NP1) for *K. pneumoniae* (DM4299) and *P. aeruginosa* (PA23376) and up to 1.1 cm for PLGA50/50-NP6 using the same strains. Lowest activity for PLGA 50/50-NP6 was observed for *E. coli* (16027R Gram-negative) and *S. saprophyticus* (SS49453 Gram-positive) with values of 0.9 and 0.6 cm, respectively. For PLGA75/25-NP1, the lowest values of 0.3 cm was observed for Gram-positive *S. saprophyticus* (SS49907) and 0.2 cm for Gram-negative *E. coli* (16027R). Both the PLGA polymers with 1 wt % AgNPs showed no antimicrobial activity for following strains: *S. saprophyticus* (SSBAA750 and SS49453), *E. coli* (16027R), and *P. aeruginosa* (PA23155). Scaffolds that contained 3 wt % of AgNPs or more, showed equal antibacterial properties for some strains when compared to free AgNPs (Table II). It is important to keep maximal antimicrobial activity with possible minimal concentration of AgNPs inside the polymeric matrix and an incorporation of 3 wt % of AgNPs was also compatible with fibroblasts, while they showed high antibacterial properties. Moreover, PLGA75/25 polymer with

Table I. YM, Ultimate Tensile Strength, and Ultimate Tensile Strain of Different Nanofibrous Scaffolds

Scaffold	YM (MPa)	Ultimate tensile strength (MPa)	Ultimate tensile strain (%)
PLGA50/50	58.00 ± 8.31	1.65 ± 0.11	24.08 ± 3.36
PLGA50/50-NP1	37.27 ± 5.99	1.26 ± 0.20	15.34 ± 1.91
PLGA50/50-NP3	34.01 ± 10.90	1.73 ± 0.05	14.29 ± 0.81
PLGA50/50-NP6	21.79 ± 11.58	0.71 ± 0.11	11.19 ± 1.50
PLGA75/25	191.29 ± 14.85	4.83 ± 0.27	50.91 ± 6.63
PLGA75/25-NP1	149.94 ± 15.29	4.59 ± 0.42	62.98 ± 6.82
PLGA75/25-NP3	135.44 ± 11.61	2.91 ± 0.08	12.84 ± 1.21
PLGA75/25-NP6	112.83 ± 4.34	2.55 ± 0.95	23.50 ± 3.14

Table II. Antibacterial Zone of Inhibition of Different Electrospun Scaffolds Compared to AgNPs Itself

	Zone of inhibition (cm)							
	K. pneumoniae	*E. coli*	*P. aeruginosa*		*S. saprophyticus*			
Material/scaffold	DM4299	16027R	PA23155	PA23376	SS49907	SS15305	SSBAA750	SS49453
	(–)	(–)	(–)	(–)	(+)	(+)	(+)	(+)
Silver NPs	1.8–1.9	0.8	0.8	2.1	2.3	1.6	1.1–2.4	1.4–1.5
PLGA50/50-NP0	0	0	0	0	0	0	0	0
PLGA50/50-NP1	0.5	0	0	0.5	0.5	0.4	0	0
PLGA50/50-NP3	0.5	0.8	0.8–0.9	0.4–0.5	0.5	0.4–0.5	0.7–0.9	0.3–0.4
PLGA50/50-NP6	1–1.1	0.9	1.0	1–1.1	1.1–1.2	1–1.1	0.9–1.1	0.6–0.7
PLGA75/25-NP0	0	0	0	0	0	0	0	0
PLGA75/25-NP1	0.4–0.5	0	0	0.5	0.3	0.3–0.4	0	0
PLGA75/25-NP3	0.5–0.7	0.2–0.4	0.4	0.3–0.6	0.4	0.4	0.5	0.3–0.4
PLGA75/25-NP6	0.7	0.3–0.6	0.4	0.6–0.9	0.4–0.5	0.4–0.5	1–1.1	0.3–0.4

All values are measured with regard to clean areas around the specimen.

3 wt % of AgNPs showed sufficient mechanical properties similar to native skin, and are more suitable compared to other scaffolds of this study, to apply as a wound graft for regeneration of the skin.

DISCUSSION

AgNPs provide large surface area and are a good source of silver ions, such that they can act like growth-inhibitors against the microorganisms. Recent discoveries showed direct anti-inflammatory properties of AgNPs with ability to enhance the healing process of living tissues.[36] Use of AgNPs in wound healing have also been demonstrated with better collagen alignment along the treated wound compared to the control group.[3,37,38] Electrospinning technique allows for the fabrication of nanofibrous structures from a variety of polymers and allow for the incorporation of AgNPs within the scaffold. Additionally, synthetic aliphatic block polymers like PLGA introduces biodegradability which is essential for the treatment of wounds without the need of multiple surgeries. Nanofibrous morphology of the scaffolds are especially interesting in the field of skin tissue engineering due to its ability to mimic the natural ECM. Random alignment of fibers, high porosity, and extraordinary surface-to-volume ratio induces cells to proliferate and assist in tissue regeneration. The biodegradability of matrix polymer allows for its replacement by natural ECM during the wound healing process.

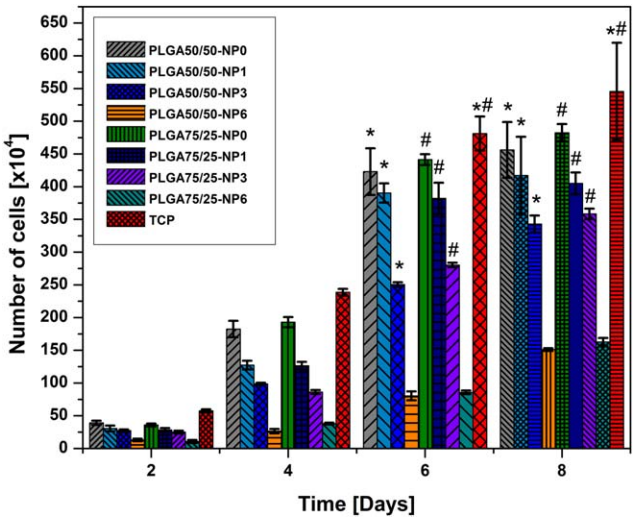

Figure 8. Proliferation of HDF determined by AlamarBlue test (* Significant against cell proliferation on PLGA50/50-NP6 scaffold at $P \leq 0.05$; # Significant against cell proliferation on PLGA75/25-NP6 scaffold at $P \leq 0.05$). [Color figure can be viewed in the online issue, which is available at wileyonlinelibrary.com.]

Analysis of the morphology of the prepared scaffolds by AFM, showed correlation between surface roughness and wettability. Addition of AgNPs into the polymer solution might have increased the electrical conductivity of the solution, which influenced the electrospinning process resulting in the decrease of fiber diameters. Fiber diameters changed drastically after addition of even smaller amounts of AgNPs, though the differences in fiber diameter was not significant among the different PLGA-NPs scaffolds. Lower porosity of densely packed fibrous mesh reduced the roughness of the scaffold, and our results of wettability was in agreement to the results of the AFM studies.[39,40]

Mechanical property evaluations of the prepared scaffolds showed that the ultimate tensile stress of PLGA75/25-NP3 was similar to those of the ultimate tensile stress values of the human skin tissue. Human abdomen and thorax were reported to have a UTS of 2–15 MPa[41] while forehead and arm are suggested to have a UTS of 5.7–12.6 MPa.[42] The nanocomposites prepared during this study had UTS values of approximately of 1–5 MPa, and are suggested for wound dressing applications. YM of the scaffolds decreased with the addition of AgNPs, but it was still comparable to the YM of natural skin tissue.[42,43] Decrease in the stiffness of the scaffolds is due to the presence of AgNPs which act as a lubricant within the polymeric matrix, mobilizing the fibers to move between each other. At the same time, the ratio of lactide : glycolide is known to influence the

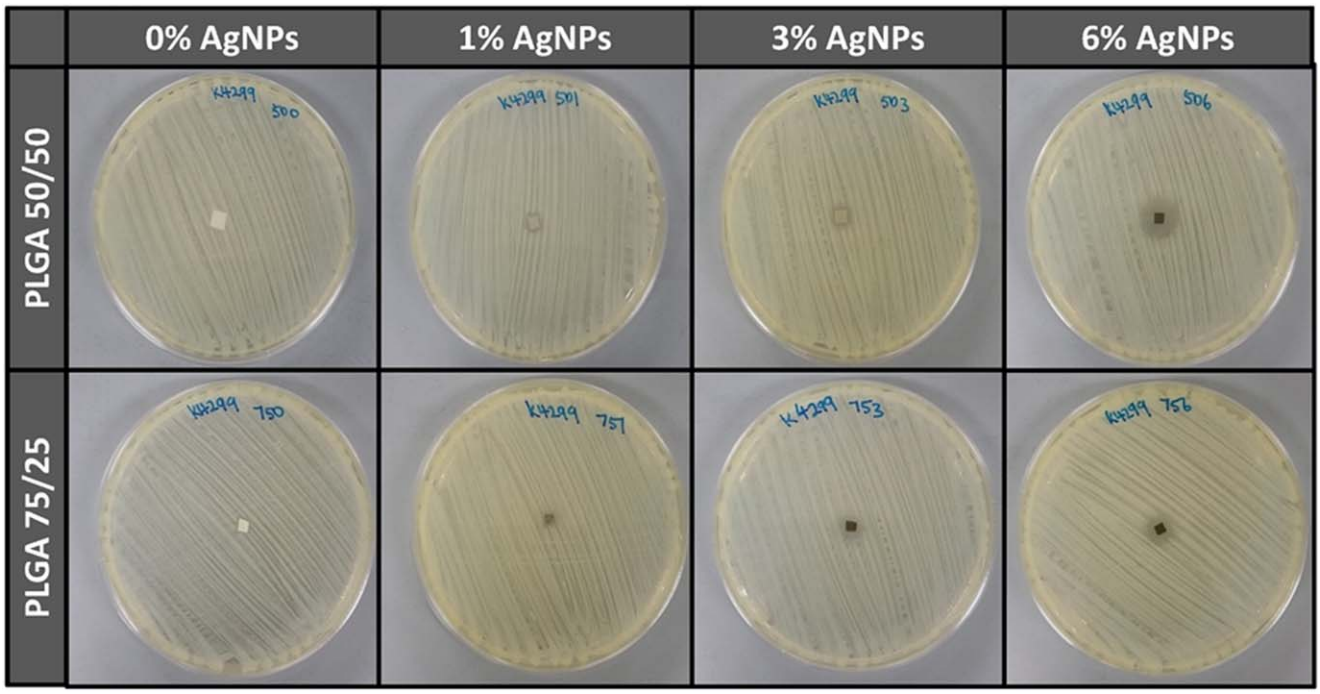

Figure 9. Antibacterial activity of the different electrospun scaffolds against *P. aeruginosa.* [Color figure can be viewed in the online issue, which is available at wileyonlinelibrary.com.]

ultimate stress, since the amorphous glycolide impart lower mechanical properties to the scaffold.[44] In fact, the incorporation of AgNPs to the polymer matrix, did not help to strengthen the scaffold, and a mere integration of the polymer with the metallic particles might have occurred and it act like breaking points within the polymer chains. Increase in the amount of AgNPs within the polymer matrix, increased the chances of fiber breakages when mechanical stress was applied and this was confirmed from the reduced values of ultimate tensile stress and strain obtained for 6 wt % AgNPs containing PLGA scaffolds.

Spectroscopic measurements showed the interaction between polymer matrix and AgNPs, with increased absorbance values was obtained with increased incorporation of AgNPs. No changes in matrix properties have been measured which suggests no specific bonding between the components and this allows the silver to be present in its ionic form. Dispersed AgNPs inside the polymeric matrix release the silver cations and introduced antibacterial activity against the Gram-negative and Gram-positive bacterial strains (*S. saprophyticus, K. pneumoniae, P. aeruginosa,* and *E. coli*) used in this study. Since the amount of silver ions released is proportional to the concentration of the AgNPs incorporated within the polymer matrix, the antimicrobial activity also increased, and this was highly observed for the PLGA-NP6 scaffolds.

Antibacterial activity of the electrospun nanofibers incorporated with AgNPs was also compared with the antibacterial activity of pure AgNP powder, used as the positive control. The antimicrobial properties of AgNPs are still not fully understood, nevertheless a number of researchers have investigated the interactions between bacteria or fungus with AgNPs or Ag ions. Antimicrobial mechanism of AgNPs is complex and it involves multi-site reaction involving cell membrane as well as organelles. AgNPs anchor itself to cell membrane and infiltrate causing changes in its permeability eventually resulting in cell death. AgNPs are also known to have a tendency to agglomerate onto the membrane of the bacteria.[25,45] Other group of researchers focused on the creation of free radicals by AgNPs and its interaction with cell organelles was suggested. Electron spin resonance spectroscopy studies revealed that the AgNPs released free radicals when in contact with bacteria further leading to the infiltration of cell membrane, making it porous and finally cell death occurred. Silver ions released from AgNPs interact with thiol groups of bacteria cells, causing the inactivation of vital enzymes thus inhibiting the cell metabolism rate.[46,47] The differences in the antibacterial activity between the pure AgNPs powder and the scaffold, is mainly related to the mode of existence of Ag, whereby the silver was dispersed within the nanoscale fibrous material for the electrospun scaffolds, while the concentrated AgNPs powder itself functioned as the positive controls. About 1 mg of Ag powder was used to test on all strains simultaneously with the prepared scaffolds. Free AgNPs at a concentration of 1 mg, showed better antibacterial properties than the AgNP containing scaffolds. However, lesser amounts of AgNPs could introduce less toxicity to cells, and we observed 3 wt % AgNPs within PLGA as the optimal scaffold with good antibacterial properties, most likely due to the uniform distribution of AgNPs within the polymer matrix. At the same time, PLGA composites containing 6 wt % of AgNPs had similar antibacterial activity as 1 mg of pure agglomerated AgNP powder itself. Nevertheless, the cell proliferation on scaffolds containing 6 wt % of AgNPs is minimal suggesting some toxicity of AgNPs at higher concentrations. The presence of 3 wt % of AgNPs in

PLGA matrix showed higher biocompatibility with HDF, with positive attribute towards antibacterial properties. This results are in accordance with the results demonstrated by Rinaldi *et al.*[48] where they combined AgNPs with PLGA shells in the form of composite nanocapsules. The presence of 3 wt % AgNPs inside the nanospheres showed high antimicrobial properties. However, the isolation of antimicrobial agents within the nanospheres limits the ability of such system as wound dressings. Mohiti-Asli *et al.*[49] showed decrease in the viability of HDF and human epidermal keratinocytes on poly(L-lactic acid) scaffolds, when the release of silver ion exceeded some typical value and it was specific for each type of cells. Similarly, Chaubey *et al.*[4] revealed that an increase in the level of AgNPs above certain levels decreased the viability of Hela (cervical cancer cells) and MCF-7 (breast cancer cells). Though the toxicity of AgNPs have been investigated previously, there is still no conclusion regarding the mechanism of the metabolism process occurring inside the human cells. Few research groups suggest that the size and concentration of silver particles are the main factors involved in this process.[50] Our results shows that an optimal amount of 3 wt % of AgNPs was sufficient to produce biodegradable PLGA composite scaffolds with suitable mechanical, antibacterial, and cytotoxic properties to functional as a bioengineered skin graft for regeneration of wounds.

CONCLUSIONS

Various biodegradable and non-biodegradable materials have been tested as carriers for AgNPs or silver ions, thus improving the antibacterial properties of the developed scaffolds. The integration of AgNPs within the PLGA matrix was carried out during this study creating nanofibrous scaffolds with mechanical properties comparable to various skin tissues. The antibacterial activity of the scaffolds were evaluated against *P. aeruginosa*, *K. pneumoniae, S. saprophyticus,* and *E. coli,* and the scaffolds were found to inhibit the bacterial growth, which was also dependent on the concentration of AgNPs incorporated within the scaffold. However, high concentrations of AgNPs inside the polymeric matrix showed toxicity against HDF lead us to the conclusion that the antibacterial activity must be compromised with the cytotoxicity of biodegradable antibacterial nanofibrous materials and the concentration of AgNPs must be adjusted to the level which preserves the antibacterial activity with minimal toxicity to cells. The electrospun PLGA75/25 incorporated with 3 wt % AgNPs had sufficient mechanical properties, induced cell proliferation and have sufficient antibacterial activity to be used as wound dressing for treatment of skin injuries, burns or chronic wounds.

ACKNOWLEDGMENTS

RL and GTLE thank the funding support from National Medical Research Council's Co-operative Basic Research Grant (NMRC/CBRG/0048/2013). The authors declare no conflict of interest.

REFERENCES

1. Tseng, Y. Y.; Liao, J. Y.; Chen, W. A.; Kao, Y. C.; Liu, S. J. *Nanomedicine* **2014**, *9*, 77.
2. Wei, J.; Hu, J.; Li, M.; Chen, Y.; Chen, Y. *RSC Adv.* **2014**, *4*, 28011.
3. Almajhdi, F. N.; Fouad, H.; Khalil, K. A.; Awad, H. M.; Mohamed, S. H. S.; Elsarnagawy, T.; Albarrag, A. M.; Al-Jassir, F. F.; Abdo, H. S. *J. Mater. Sci.-Mater. Med.* **2014**, *25*, 1045.
4. Chaubey, N.; Sahoo, A. K.; Chattopadhyay, A.; Ghosh, S. S. *Biomater. Sci.* **2014**, *2*, 1080.
5. Gungor-Ozkerim, P. S.; Balkan, T.; Kose, G. T.; Sarac, A. S.; Kok, F. N. *J. Biomed. Mater. Res. Part A* **2014**, *102*, 1897.
6. Jiang, J.; Xie, J.; Ma, B.; Bartlett, D. E.; Xu, A.; Wang, C. H. *Acta Biomater.* **2014**, *10*, 1324.
7. Wang, H. L.; Li, Y. N.; Jiang, S. W.; Zhang, P.; Min, S.; Jiang, S. T. *J. Appl. Polym. Sci.* **2014**, *131*, 8.
8. Huang, Z.-M.; Zhang, Y. Z.; Kotaki, M.; Ramakrishna, S. *Compos. Sci. Technol.* **2003**, *63*, 2223.
9. World Health Organization Report. *Prevention of Hospital-Acquired Infections. A Practical Guide.* 2nd ed. **2002**, WHO/CDS/CSR/EPH/2002.12.
10. Mansbridge, J. *J. Biomater. Sci. Polym. Ed.* **2008**, *19*, 955.
11. Lee, S. B.; Kim, Y. H.; Chong, M. S.; Hong, S. H.; . Lee, Y. M. *Biomaterials* **2005**, *26*, 1961.
12. Liu, P.; Deng, Z.; Han, S.; Liu, T.; Wen, N.; Lu, W.; Geng, X.; Huang, S.; Jin, Y. *Artif. Organs* **2008**, *32*, 925.
13. Cui, W.; Zhu, X.; Yang, Y.; Li, X.; Jin, Y. *Mater. Sci. Eng.: C* **2009**, *29*, 1869.
14. Altankov, G.; Thom, V.; Groth, T.; Jankova, K.; Jonsson, G.; Ulbricht, M. *J. Biomed. Mater. Res.* **2000**, *52*, 219.
15. Ma, G.; Yang, D.; Wang, K.; Han, J.; Ding, S.; Song, G.; Nie, J. *J. Appl. Polym. Sci.* **2010**, *118*, 3619.
16. Dahlin, R. L.; Kasper, F. K.; Mikos, A. G. *Tissue Eng. Part B: Rev.* **2011**, *17*, 349.
17. Srinivasan, S.; Jayakumar, R.; Chennazhi, K. P.; Levorson, E.; Mikos, A.; Nair, S. In Biomedical Applications of Polymeric Nanofibers; Jayakumar, R., Nair, S., Eds.; Springer Berlin: Heidelberg, **2012**; Vol. 246, p 1.
18. Smith, L. A.; Liu, X.; Ma, P. X. *Soft Matter* **2008**, *4*, 2144.
19. Lu, L.; Peter, S. J.; Lyman, M. D.; Lai, H. L.; Leite, S. M.; Tamada, J. A.; Uyama, S.; Vacanti, J. P.; Langer, R.; Mikos, A. G. *Biomaterials* **2000**, *21*, 1837.
20. Houchin, M. L.; Topp, E. M. *J. Pharm. Sci.* **2008**, *97*, 2395.
21. Ger, T. R.; Huang, H. T.; Huang, C. Y.; Hu, K. S.; Lai, J. Y.; Chen, J. Y.; Lai, M. F. *J. Appl. Phys.* **2014**, *115*, 3.
22. Shen, L. K.; Fan, K. H.; Wu, T. L.; Huang, H. M.; Leung, T. K.; Chen, C. J.; Chang, W. J. *J. Polym. Eng.* **2014**, *34*, 231.
23. Khalil Abdelrazek Khalil, H. F.; Elsarnagawy, T.; Almajhdi, F. N. *Int. J. Electrochem. Sci.* **2013**, *8*, 3483.
24. Xu, X.; Yang, Q.; Bai, J.; Lu, T.; Li, Y.; Jing, X. *J. Nanosci. Nanotechnol.* **2008**, *8*, 5066.
25. Sondi, I.; Salopek-Sondi, B. *J. Colloid Interface Sci.* **2004**, *275*, 177.
26. Schneider, C. A.; Rasband, W. S.; Eliceiri, K. W. *Nat. Methods* **2012**, *9*, 671.

27. Yarin, A. L.; Koombhongse, S.; Reneker, D. H. *J. Appl. Phys.* **2001**, *90*, 4836.
28. Angammana, C. J.; Jayaram, S. H. In IEEE-IAS Annual Meeting; Edmonton, Alberta: Canada, 5–9 Oct. **2008**.
29. Taheri, S.; Baier, G.; Majewski, P.; Barton, M.; Forch, R.; Landfester, K.; Vasilev, K. *J. Mater. Chem. B* **2014**, *2*, 1838.
30. D'Avila Carvalho Erbetta, R. J. A. C.; Magalhães Resende, J.; Fernando de Souza Freitas, R.; Geraldo de Sousa, R. *J. Biomater. Nanobiotechnol.* **2011**, *3*, 208.
31. Bhui, D. K.; Bar, H.; Sarkar, P.; Sahoo, G. P.; De, S. P.; Misra, A. *J. Mol. Liquids* **2009**, *145*, 33.
32. Kunkely, H.; Vogler, A. *Inorg. Chem. Commun.* **2001**, *4*, 692.
33. Hunt, H. D.; Simpson, W. T. *J. Am. Chem. Soc.* **1953**, *75*, 4540.
34. Shin, H. J.; Lee, C. H.; Cho, I. H.; Kim, Y.-J.; Lee, Y.-J.; Kim, I. A.; Park, K.-D.; Yui, N.; Shin, J.-W. *J. Biomater. Sci., Polym. Ed.* **2006**, *17*, 103.
35. Yao, J.; Bastiaansen, C.; Peijs, T. *Fibers* **2014**, *2*, 158.
36. Nadworny, P. L.; Wang, J.; Tredget, E. E.; Burrell, R. E. *Nanomed.: Nanotechnol. Biol. Med.* **2008**, *4*, 241.
37. Tse, C.; Zohdy, M. J.; Ye, J. Y.; O'Donnell, M.; Lesniak, W.; Balogh, L. *Nanomed.: Nanotechnol. Biol. Med.* **2011**, *7*, 97.
38. Inbathamizh, L.; Ponnu, T. M.; Mary, E. J. *J. Pharm. Res.* **2013**, *6*, 32.
39. Kubiak, K. J.; Wilson, M. C. T.; Mathia, T. G.; Carval, P. *Wear* **2011**, *271*, 523.
40. Wu, N.; Jiao, Y.; Chen, L. *J. Eng. Fibers Fabrics* **2013**, *8*, 1.
41. Silver, F. H.; Freeman, J. W.; DeVore, D. *Skin Res. Technol.* **2001**, *7*, 18.
42. Jacquemoud, C.; Bruyere-Garnier, K.; Coret, M. *J. Biomech.* **2007**, *40*, 468.
43. Ní Annaidh, A.; Bruyère, K.; Destrade, M.; Gilchrist, M. D.; Otténio, M. *J. Mech. Behav. Biomed. Mater.* **2012**, *5*, 139.
44. McDonald, P. F.; Geever, L. M.; Lyons, J. G.; Higginbotham, C. L. *Polym.-Plast. Technol. Eng.* **2010**, *49*, 678.
45. Prabhu, S.; Poulose, E. *Int. Nano Lett.* **2012**, *2*, 1.
46. Kim, J. S.; Kuk, E.; Yu, K. N.; Kim, J.-H.; Park, S. J.; Lee, H. J.; Kim, S. H.; Park, Y. K.; Park, Y. H.; Hwang, C.-Y.; Kim, Y.-K.; Lee, Y.-S.; Jeong, D. H.; Cho, M.-H. *Nanomed.: Nanotechnol. Biol. Med.* **2007**, *3*, 95.
47. Danilczuk, M.; Lund, A.; Sadlo, J.; Yamada, H.; Michalik, J. *Spectrochim. Acta Part A: Mol. Biomol. Spectrosc.* **2006**, *63*, 189.
48. Rinaldi, S.; Fortunati, E.; Taddei, M.; Kenny, J. M.; Armentano, I.; Latterini, L. *J. Appl. Polym. Sci.* **2013**, *130*, 1185.
49. Mohiti-Asli, M.; Pourdeyhimi, B.; Loboa, E. G. *Acta Biomater.* **2014**, *10*, 2096.
50. Gliga, A.; Skoglund, S.; Odnevall Wallinder, I.; Fadeel, B.; Karlsson, H. *Part. Fibre Toxicol.* **2014**, *11*, 11.